

# **Modulo: New paradigm**

**Laura Magrini & Daniele Galli**  
**Osservatorio Astrofisico di Arcetri**

# Initial conditions

1. Homogeneous spherical cold neutral gas cloud with two initial masses:  $M=10^9 M_{\odot}$  and  $10^{11} M_{\odot}$ . The gas temperature can assume one of three possible values: 20, 25, 30 K; and the gas density  $n_{\text{HI}}$  two values:  $1 \text{ cm}^{-3}$  and  $10 \text{ cm}^{-3}$ .

2. The volume density of the gas is:

$$\rho_{\text{HI}} = m_{\text{H}} \mu n_{\text{HI}} ,$$

the radius of the gas sphere is:

$$R_{\text{HI}} = [3M_{\text{HI}}/(4\pi\rho_{\text{HI}})]^{1/3} ,$$

and the surface density of the gas is:

$$\Sigma_{\text{HI}} = \rho_{\text{HI}} R_{\text{HI}} ,$$

where  $m_{\text{H}}$  is the mass of a hydrogen atom,  $\mu$  is the molecular weight of the gas, in this case  $\mu = 1.2$  to take neutral helium into account, and  $n_{\text{HI}}$  is the HI number density.

# Initial molecular cloud conditions

The clouds have three possible values of number density  $n_{\text{H}_2}$ :

Diffuse:  $n_1 = 10^3 \text{ cm}^{-3}$

Compact:  $n_2 = 5 \times 10^4 \text{ cm}^{-3}$

Hyper dense:  $n_3 = 10^6 \text{ cm}^{-3}$

From the cloud densities, we compute their free-fall collapse time:

$$t_{\text{ff}} = \sqrt{3\pi/32G\rho_{\text{gas}}}$$

# Characteristics of proto-galaxies

Density:  
 $1-10 \text{ cm}^{-3}$

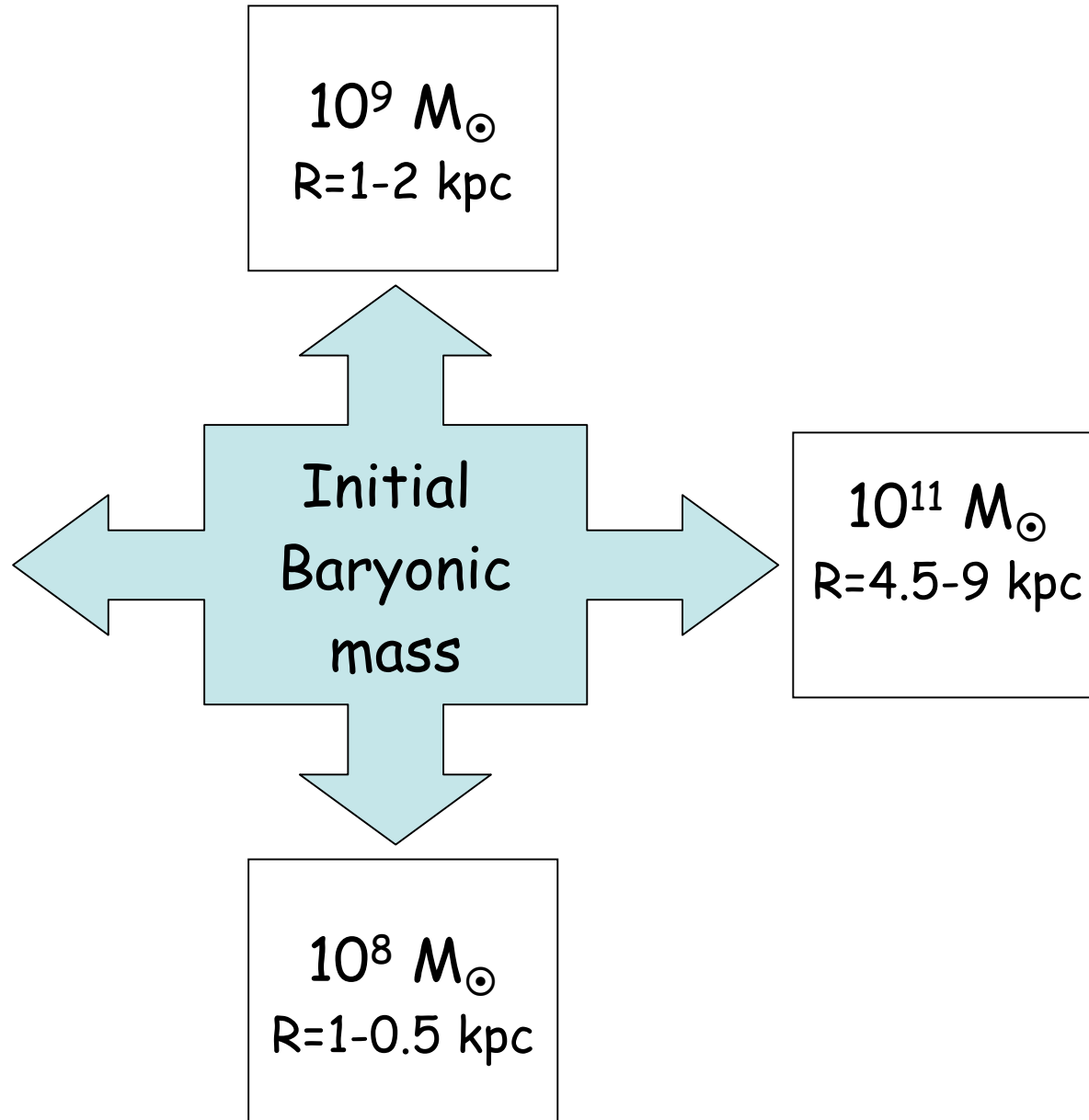
$10^9 M_{\odot}$   
 $R=1-2 \text{ kpc}$

$10^7 M_{\odot}$   
 $R=0.5-0.2 \text{ kpc}$

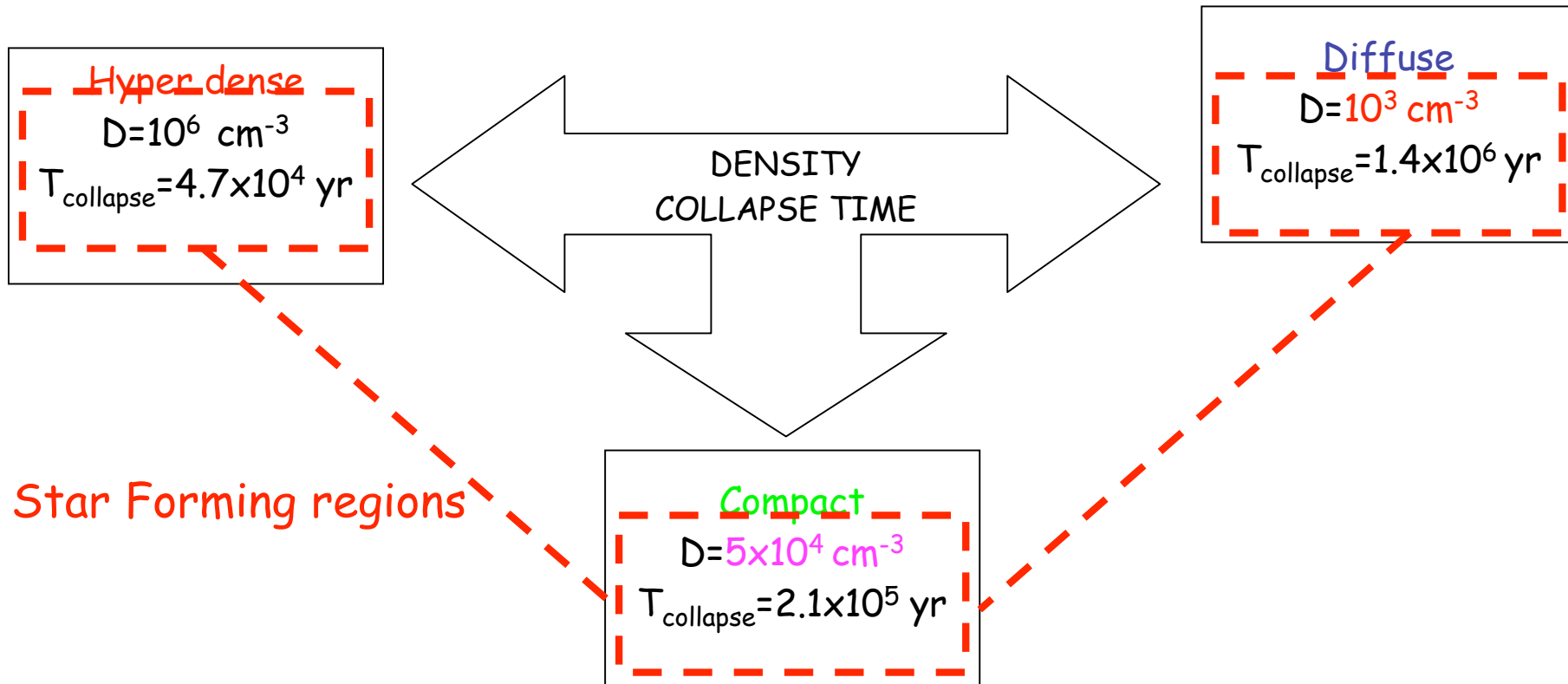
Initial  
Baryonic  
mass

$10^{11} M_{\odot}$   
 $R=4.5-9 \text{ kpc}$

$10^8 M_{\odot}$   
 $R=1-0.5 \text{ kpc}$



# Clouds characteristics



# The phase transformations:

## 1. From atomic gas to clouds:

Initially the  $H_2$  fraction is zero, for a given metallicity  $Z$  and  $\Sigma_{\text{gas}} = \Sigma_{\text{HI}} + \Sigma_{\text{H}_2}$ , the fraction of gas in  $H_2$  can be calculated with the Krumholz, McKee, & Tumlinson (KMT) formulation:

$$f_{\text{H}_2} = f(Z, \Sigma_{\text{gas}}),$$

namely  $M_{\text{H}_2} = f_{\text{H}_2} M_{\text{gas}}$ , where  $M_{\text{gas}} = M_{\text{HI}} + M_{\text{H}_2}$ .

## 2. From molecular clouds to stars:

The star-formation rate SFR surface density is calculated:

$$d\Sigma^*/dt = \Sigma_{\text{gas}} f_{\text{H}_2} \epsilon / \tau_{\text{ff(GMC)}}$$

# The equations of the multiphase model:

Star formation

$$\frac{ds_{1,D}}{dt} = H_{1,D}c_D^2 + a_{1,D}c_Ds_{2,D} - D_{1,D},$$

$$\frac{ds_{2,D}}{dt} = H_{2,D}c_D^2 + a_{2,D}c_Ds_{2,D} - D_{2,D},$$

$$\frac{dg_D}{dt} = -\mu_D g_D^n + a'_D c_D s_{2,D} + H'_D c_D^2 + W_D + fg_H,$$

Infall

Cloud formation

$$\frac{dc_D}{dt} = \mu_D g_D^n - (a_{1,D} + a_{2,D} + a'_D)c_D s_{2,D} - (H_{1,D} + H_{2,D} + H'_D)c_D^2$$

$$\frac{dr_D}{dt} = D_{1,D} + D_{2,D} - W_D$$

# Modulo in the multiphase model

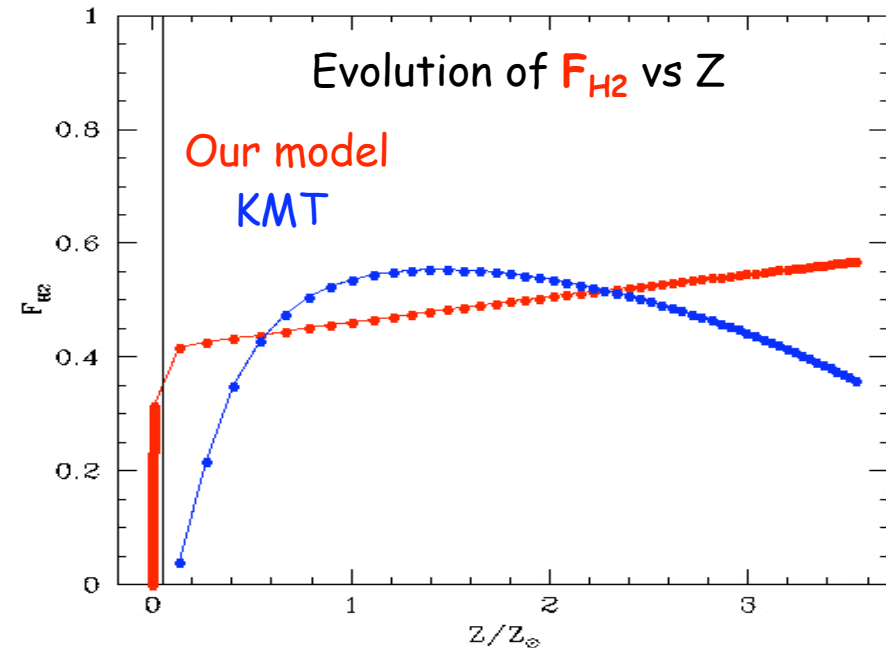
## Cloud formation

- The molecular cloud fraction by KMT is not directly introduced, but it is compared with the molecular cloud fraction obtained in our model: molecular clouds are formed from atomic gas collapse, following the relation

$$dF_{H_2}/dt = \varepsilon F_{HI}^{1.5}$$

The final result for the evolution of the molecular cloud fraction evolution is very similar to the KMT fractions, with several advantages:

- Easier to compute
- Applicable also at low metallicity
- Applicable at any  $\Sigma_{gas}$





# Modulo in the multiphase model

## Star formation

- The three different molecular cloud density regimes give us three star formation global efficiency:

$$\Sigma_{\text{gas}} f_{\text{H}_2} \epsilon / \tau_{\text{ff(GMC)}}$$

- While  $\epsilon$  is constant,  $\tau_{\text{ff(GMC)}}$  depends inversely on the cloud density, and thus **compact** clouds form stars more efficiently than **diffuse** clouds.

$$\frac{ds_{1,D}}{dt} = H_{1,D} c_D^2 + \epsilon$$

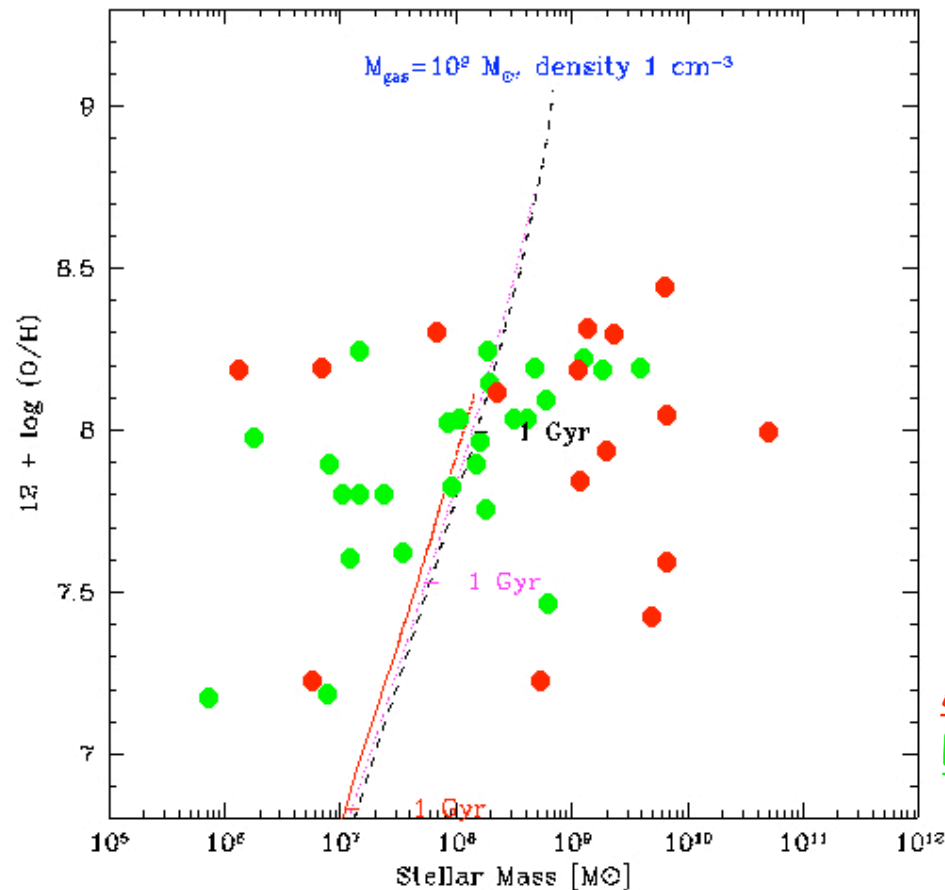
$$\frac{ds_{2,D}}{dt} = H_{2,D} c_D^2 + \epsilon$$

# The BCD sample: constraints from observations

```
# X conversion factor = 3.000e+20 cm^-2 (K km/s)^-1
```

| #              | Name | Distance<br>(Mpc) | 12+<br>logOH | <B-K> | <LK><br>(Msun) | Diameter<br>NED<br>(kpc) | LogMstar<br>min avg<br>(Msun) | HI<br>Sigma(HI)<br>(cm^-2) (Msun/pc^2) | Flag | CO<br>Sigma(H2)<br>(cm^-2) (Msun/pc^2) | Flag      | SFR<br>(Msun/<br>yr) | SFR<br>(Msun/<br>yr/kpc^2) |       |       |     |
|----------------|------|-------------------|--------------|-------|----------------|--------------------------|-------------------------------|--|------|--|-----------|----------------------|----------------------------|-------|-------|-----|
| Haro3          | 16.8 | 8.30              | 2.89         | 9.72  | 4.79           | 9.09                     | 9.35                          | 1.282e+21                              | 10.3 | m21                                    | 5.940e+20 | 9.5                  | OK                         | 1.90  | 0.106 | 13. |
| IIZw40         | 10.3 | 8.12              | 1.24         | 9.13  | 1.04           | 8.09                     | 8.34                          | 1.145e+22                              | 91.7 | m21                                    | 1.500e+20 | 2.4                  | OK                         | 3.90  | 4.610 | 13. |
| IZw18          | 13.0 | 7.19              | 1.10         | 7.71  | 0.93           | 6.51                     | 6.88                          | 4.919e+21                              | 39.4 | m21                                    | 3.000e+20 | 4.8                  | UL                         | 0.09  | 0.134 | 13. |
| Mrk209         | 5.4  | 7.81              | 2.49         | 7.83  | 1.09           | 7.29                     | 7.36                          | 1.773e+21                              | 14.2 | m21                                    | 1.350e+20 | 2.2                  | OK                         | 0.05  | 0.051 | 13. |
| Mrk33          | 24.9 | 8.45              | 3.17         | 10.09 | 6.86           | 9.59                     | 9.79                          | 5.416e+20                              | 4.3  | m21                                    | 1.863e+21 | 29.8                 | OK                         | 3.80  | 0.103 | 13. |
| Mrk71=NGC2363A | 3.4  | 7.90              | 0.12         | 7.96  | 0.81           | 6.54                     | 6.89                          | 1.545e+21                              | 12.4 | cm2                                    | 1.020e+20 | 1.6                  | UL                         | 0.11  | 0.214 | 13. |
| Mrk900         | 13.3 | 8.04              | 2.49         | 9.07  | 2.90           | 8.54                     | 8.60                          | 4.465e+20                              | 3.6  | m21                                    | 2.040e+20 | 3.3                  | OK                         | 0.09  | 0.014 | 13. |
| NGC1140        | 18.2 | 8.20              | 3.30         | 9.84  | 6.55           | 9.30                     | 9.58                          | 1.965e+21                              | 15.7 | m21                                    | 2.910e+20 | 4.7                  | OK                         | 0.82  | 0.024 | 13. |
| NGC1156        | 7.1  | 8.23              | 2.53         | 9.56  | 5.93           | 8.62                     | 9.10                          | 6.274e+20                              | 5.0  | m21                                    | 2.280e+20 | 3.7                  | OK                         | 0.19  | 0.007 | 13. |
| NGC1741        | 55.1 | 8.05              | 1.96         | 10.41 | 22.44          | 9.29                     | 9.81                          | 1.218e+21                              | 9.8  | m21                                    | 4.590e+20 | 7.4                  | OK                         | 16.00 | 0.040 | 13. |
| NGC2537        | 8.0  | 8.19              | 3.07         | 9.58  | 3.72           | 9.14                     | 9.26                          | 6.910e+20                              | 5.5  | m21                                    | 1.680e+20 | 2.7                  | OK                         | 0.15  | 0.013 | 13. |
| NGC4214        | 3.3  | 8.20              | 2.23         | 9.20  | 7.19           | 8.66                     | 8.67                          | 2.918e+20                              | 2.3  | m21                                    | 2.700e+20 | 4.3                  | OK                         | 0.13  | 0.003 | 13. |
| NGC5253        | 3.5  | 8.19              | 2.95         | 9.40  | 3.14           | 8.63                     | 9.05                          | 3.406e+20                              | 2.7  | m21                                    | 2.175e+20 | 3.5                  | OK                         | 1.40  | 0.181 | 13. |
| SBS0335-052    | 53.7 | 7.23              | 2.38         | 9.21  | 3.35           | 7.79                     | 8.72                          | 3.071e+21                              | 24.6 | m21                                    | 1.625e+21 | 26.0                 | UL                         | 1.35  | 0.154 | 13. |
| UM448          | 81.2 | 8.00              | 3.62         | 10.87 | 8.18           | 10.30                    | 10.69                         | 4.274e+21                              | 34.2 | m21                                    | 2.460e+20 | 3.9                  | OK                         | 35.20 | 0.669 | 13. |
| UM462          | 15.3 | 7.97              | 2.01         | 8.79  | 2.44           | 7.95                     | 8.20                          | 2.018e+21                              | 16.2 | m21                                    | 1.650e+20 | 2.6                  | OK                         | 0.28  | 0.060 | 13. |

# Results of the model:



The model curves correspond to different cloud density :

$10^3 \text{ cm}^{-3}$

$5 \times 10^4 \text{ cm}^{-3}$

$10^6 \text{ cm}^{-3}$

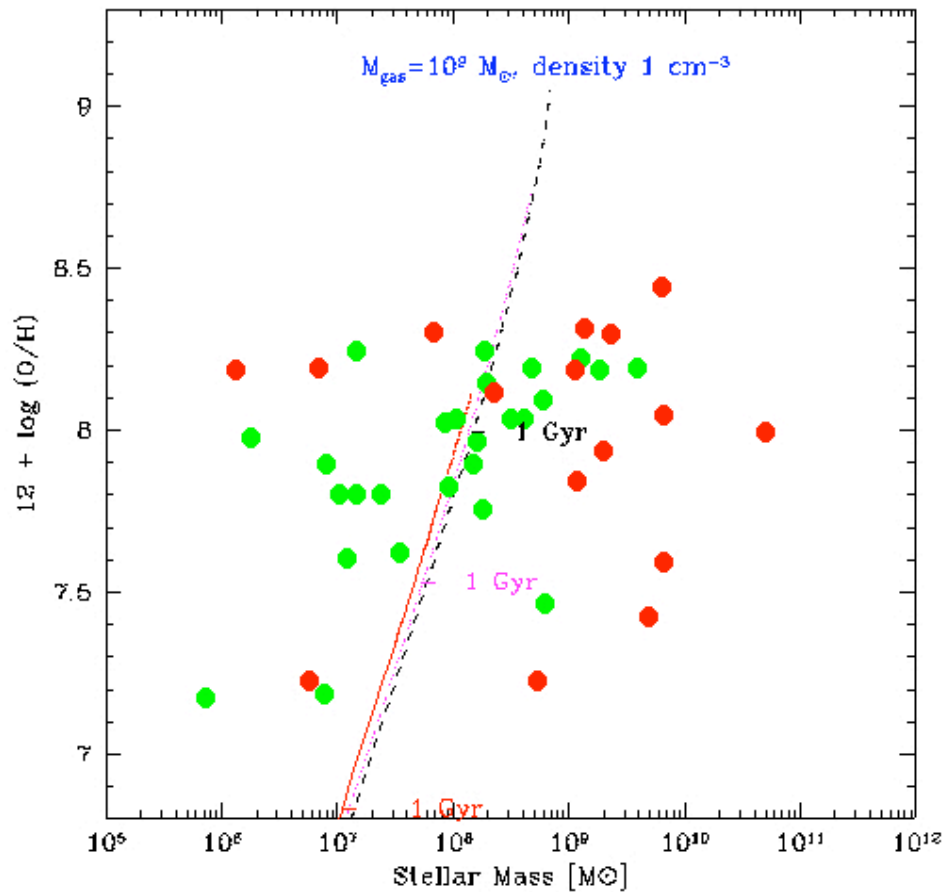
producing different time evolution

Active galaxies: SFR > 1 Msun/yr

Passive galaxies: SFR < 1 Msun/yr

Galaxies with diffuse clouds have a slower evolution than galaxies with compact clouds: at a given time in their evolution they have lower metallicity and stellar mass

However, to reproduce the mass-metallicity relationship we need to compare with a grid of model for different initial masses



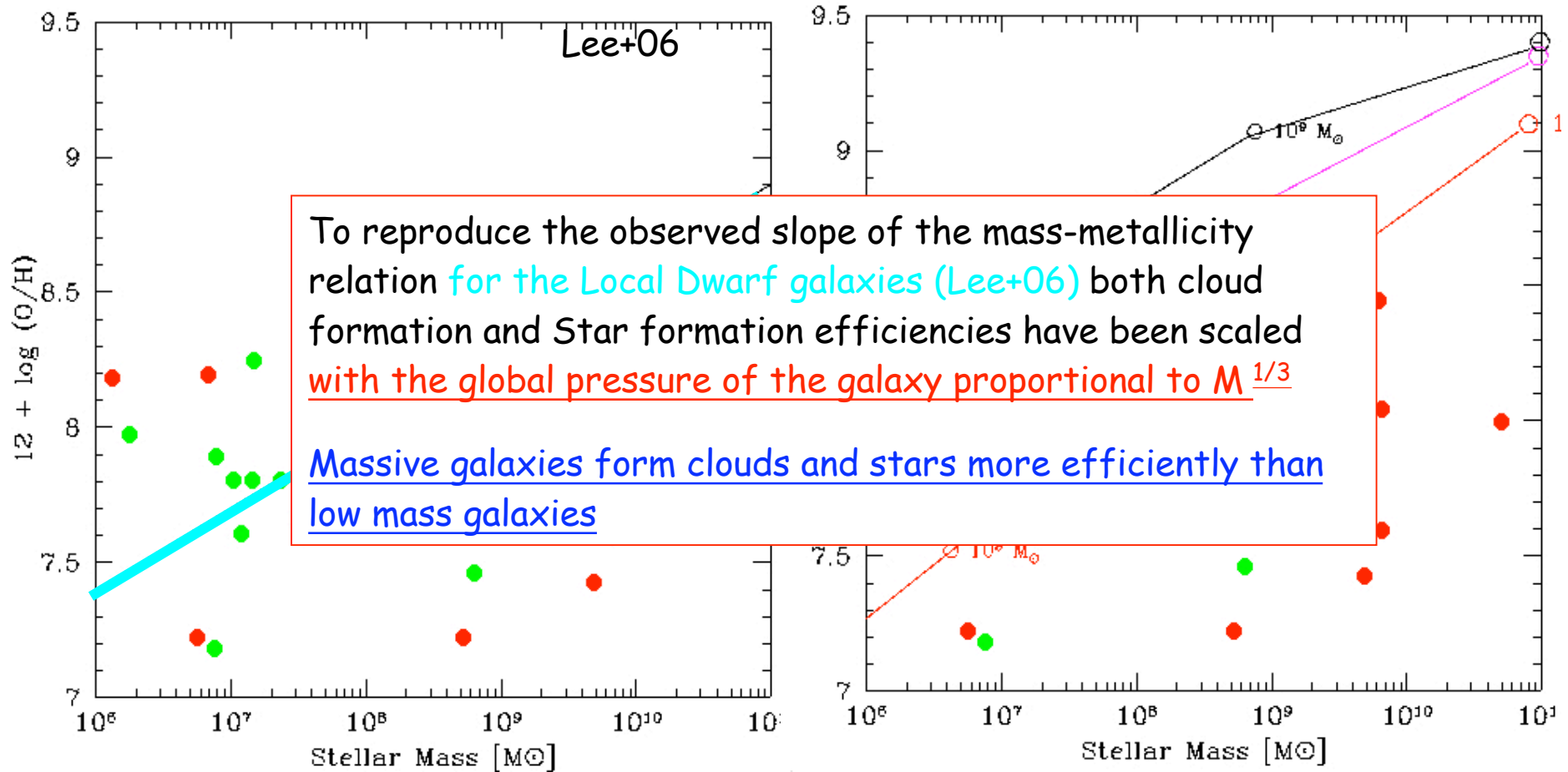
Active galaxies: SFR > 1 Msun/yr

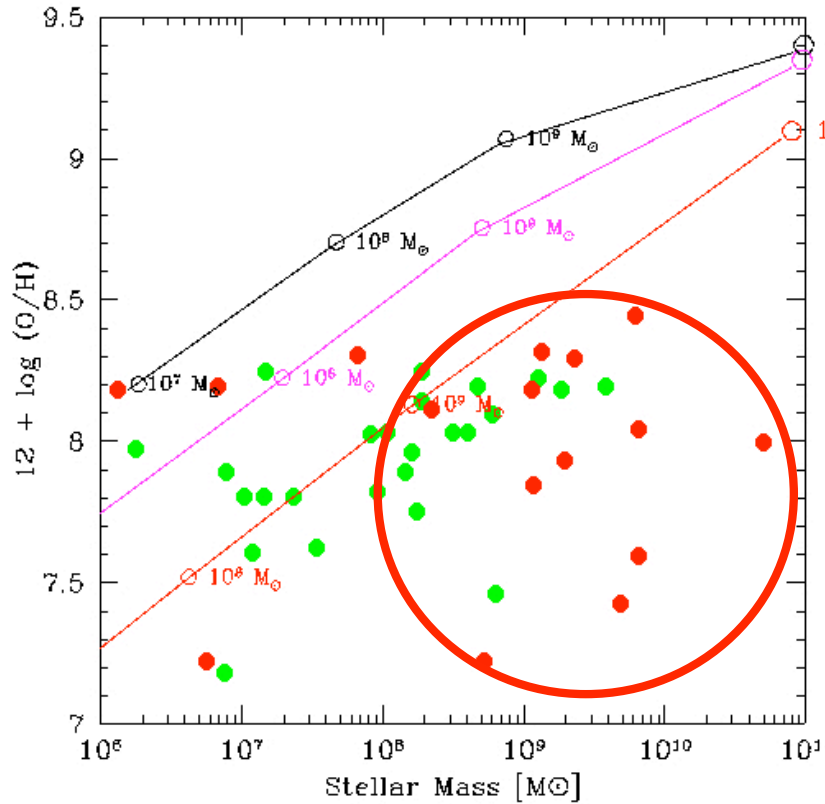
Passive galaxies: SFR < 1 Msun/yr

# Mass-metallicity relationship

Observations: **active** and **passive** galaxies and the mass-metallicity rel. from Lee+06

Models: curves at present time with three densities: **hyper-dense**, **compact**, **diffuse**

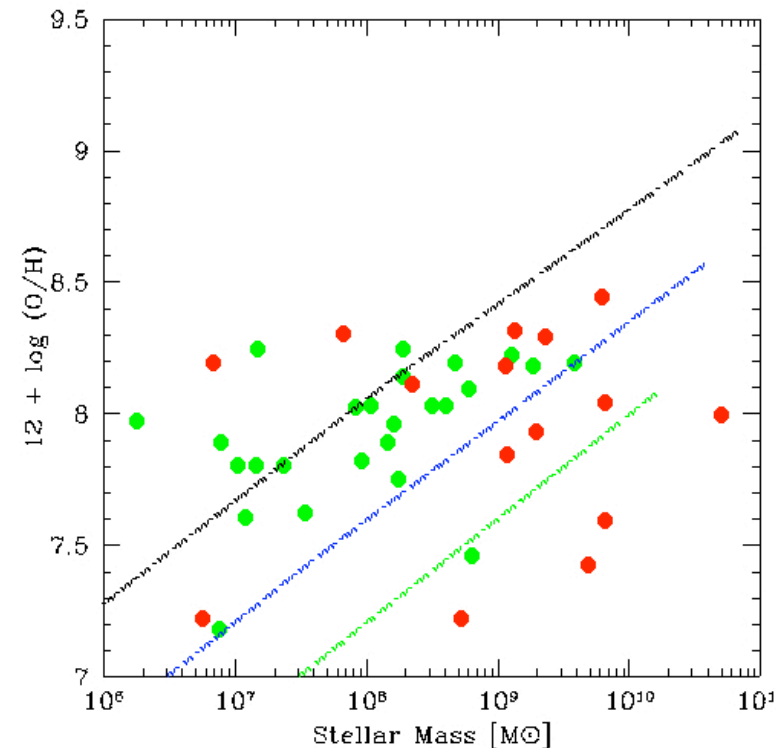




Most of the **active galaxies** do not follow the mass-metallicity relationship: they have higher stellar mass than expected for their metal content.

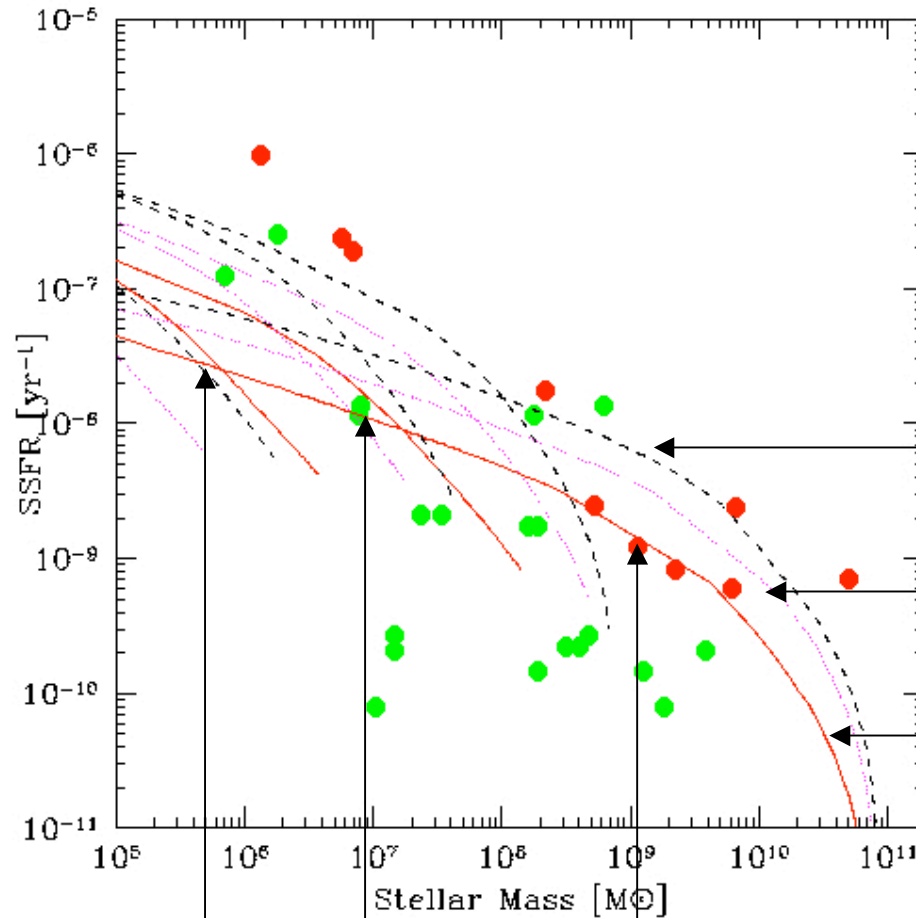
Let's fix the cloud density, i.e. the SF efficiency, and study the time evolution of the mass-metallicity relationship-->  
Active galaxies are consistent with galaxies in the early phases of their evolution

Present-time  
 Redshift  $z \sim 2$   
 $z \sim 3$



# The specific star formation rate:

in the three density cases  
and with different initial masses



Active galaxies are in better agreement with the early phases of the evolution of Ultra-dense galaxies

Ultra-dense

compact

diffuse

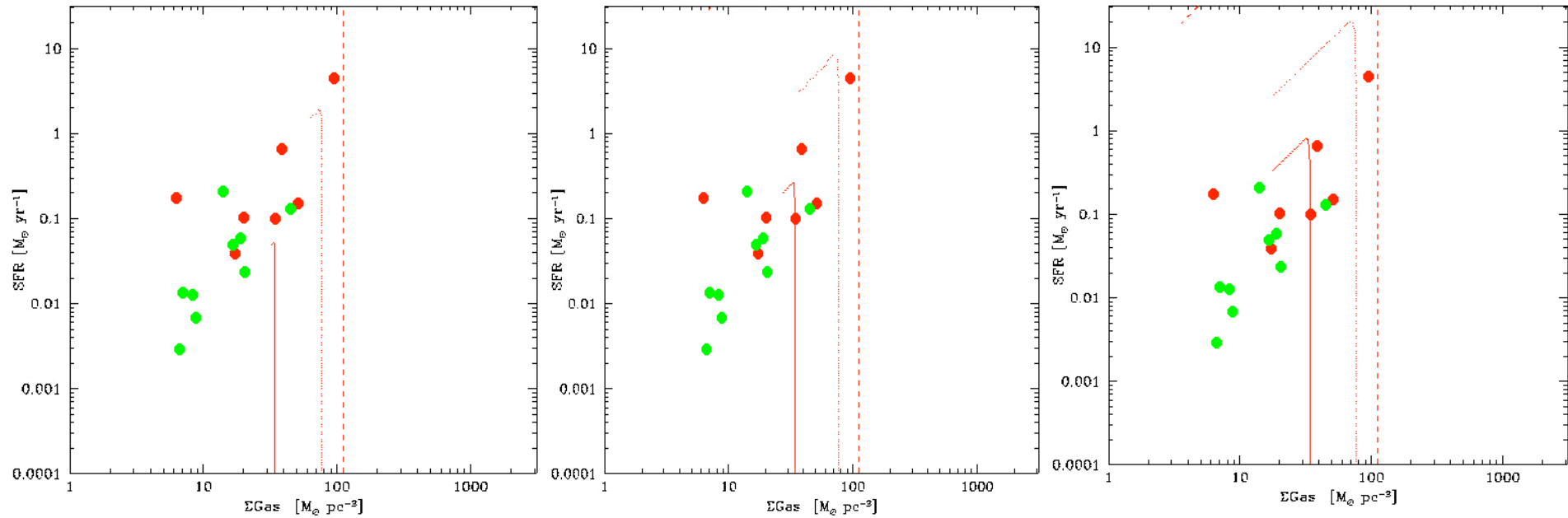
Initial mass :  $10^8$   $10^9$   $10^{11} M_{\text{sun}}$

# Kennicutt-Schmidt law

Low density

Medium density

High density

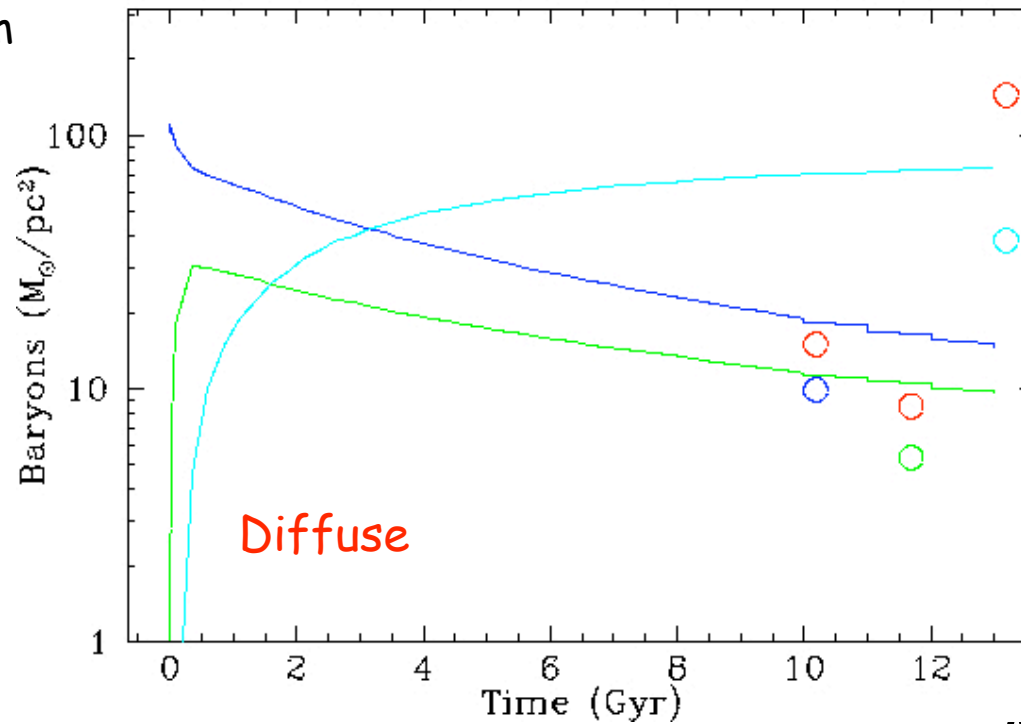




# Baryonic component evolution

Curves:  
Surface density from  
Model

Gas  
Clouds  
Stars



Circles:  
Observed surface  
Densities

Molecular clouds  
Atomic gas  
Stars

In red active  
galaxies

# Conclusions

- The multiphase model is able to reproduce the main observational constraints of the BCD sample: SFR, SSFR, mass-metallicity and Kennicutt-Schmidt relations, evolution of the baryonic Surface densities
- Different cloud densities gives different rate of evolution, and seems to associate **active galaxies** with a younger population evolving rapidly than **passive galaxies**